Eur. J. Stat. 3 (2023) 12
doi: 10.28924/ada/stat.3.12

Time Variant Wave-Signal-Amplitude Trigonometry Regression of Latitudes and Longitudes of the Belmullets of the Atlantic Ocean

Rasaki Olawale Olanrewaju[1,*], Sodiq Adejare Olanrewaju[2], Serifat Folorunsho[2], Abibat Gbemisola Dada[3]

[1]*Africa Business School (ABS), Mohammed VI Polytechnic University (UM6P), X4JH+QJR, Avenue Mohamed Ben Abdellah Regragui, Rabat 10112, Morocco*
olanrewaju_rasaq@yahoo.com
[2]*Department of Statistics, University of Ibadan, Ibadan, 900001, Nigeria*
sodiqadejare19@gmail.com, serifatf005@gmail.com
[3]*Tomia Community Junior Secondary School, Agbado-Ijaiye, Lagos State, Nigeria*
[*]*Correspondence: olanrewaju_rasaq@yahoo.com*

Abstract. This paper introduces time variant wave-signal-amplitude cosine and sine regression as an extension to wave signal Fourier function and Wave-Shape Function (WSF) model. A full-scale conditional characterization of the linear time variant wave-signal-amplitude cosine and sine model of cosine and sine function with random errors (η_i) was proposed. The associated regression coefficients were estimated via the Ordinary Least Square (OLS) technique, such that, the model wave signal, frequency, and phase were carved-out. In application to real life problem, the wave-signal-amplitude trigonometry model was applied to the real-time observations of the latitude and longitude of the wave buoys' Belmullets of the Atlantic Ocean. The full-scale real-time observations of the wave climate are the time-variant significant wave height (in metre), peak wave (in ^{o}C) and sea temperature (in ^{o}C) from 2012 to 2022.

1. Introduction

Oscillatory and wave signal (wavelike motion) have started receiving significant attention over the past century. Wave signals can be in terms of static or dynamic amplitude and frequency. Static wavy signals can be interpreted as uniform or non-uniform time-varying components of amplitude and frequency, while dynamic components can be connoted as components of amplitude and frequency without time-varying traits [1, 2, 3].

According to [4, 5], real-valued oscillatory and wave signals are mostly expressed in terms of time domain, such that they are valued as time step. This can be perceived as a useful structurization of periodic function, commonly a Fourier function or frequency domain process. Real-world wave

Received: 10 Jun 2023.
Key words and phrases. Atlantic Ocean; cosine; ordinary least square (OLS); regression; wave-signal-amplitude.

signals are sometimes not fully periodic, in such scenario, frequency spectra are used to change the time variant, see [6, 7, 8]. Consequently, this led to the concept of wavelets, as a means for bridging the lacuna between frequency and time domain. [9] theorized wavelets as a representation of repeatable structure of seismic signals. Wavelike motion function was proposed by [10] as trend- and noise-free oscillatory signal model of paired amplitude-oscillation of the realization of the form $f(t) = A(t)s(\phi(t))$, where $A \in C^1(\mathbb{R})$; $t \in \mathbb{R}$; $A \in C^1(\mathbb{R})$ is the time-varying amplitude of positive smooth function called Amplitude Modulation (AM). $\phi \in C^2(\mathbb{R})$ is the quantifiable monotonic increasing function of the signal oscillate known as phase function, and ϕ is the modulus coefficient known as Instantaneous Frequency (IF); $s(t)$ is a 1-periodic of Wave-Shape Function (WSF), (See appendix for slowing and time-varying conditions that must be satisfied).

One of the wave signal and oscillatory processes widely consider is the superimposition of Amplitude-and-Frequency-Modulated (AMFM) components, such that the signal must satisfy the Intrinsic Mode Type (IMT) condition, that is, $A(t)\cos(2\pi\phi(t))$, see [11, 12]. The wave signal of time-varying frequency and amplitude are usually faced with the lacuna of not being oscillating sinusoidal, e:g Electrocardiogram (ECG), Ocean Wave (OW), Sparse Time-Frequency (STF), Arterial Blood Pressure (ABP) etc. [13, 14, 15]. However, ECG signal represents one human heartbeat with its form and structure not related to sine wave. Statistically, non-sinusoidal are usually refer to as Wave-Shape Function (WSF, usually abbreviated as WSFv1 or WSFv2 for different types of its variation), otherwise known as 1-periodic function by mathematicians. Non-sinusoidal phenomenon via its variations of WSF model have been propounded to accommodate finer structures hidden inside the WSFv1 variant, while WSFv2 was propounded to accommodate wave-shape oscillatory model and time-varying oscillatory pattern [16, 17].

Different algorithms have been developed to study oscillatory and wave signal facing different challenges of WSFv1 and WSFv2. The notion of degree of nonlinearity and extraction of intrinsic frequency information are usually used to define sparse time-frequency via some selected algorithms [18, 19, 20].

The de-shape algorithm that was developed for the WSFv2 variant usually reduces the impinge of harmonics; such that an exponentiated nonlinear regression approach was propounded based on WSFv2 to decompose signals with time-varying wavelike motion, see [21]. In relation to recent work on wave signals and oscillation, [22, 23] presented a new method of systematic analysis of signals called Square-Wave Method (SWM). The SWM technique is based on the representation of types of signals using sum of trains square waves that are either global or local that lies solely on one time variable “t” (time). They applied the SWM to several analytical characterization signals and audio signal. [24] considered Gravitational Wave (GW) production of hybrid inflation models for an axion-like waterfall field connected to Abelian gauge fields. They deduced that the linear analysis of GW signal from the inflationary model can be within the reach of variety of foreseeable

GW experiments in terms of frequency range and signal strength. They also affirmed that the inflationary models are equivalent to primordial black hole, see [25, 26].

[27] proposed a nonlinear regression scheme to disintegrate signals into its constitutional multiple oscillatory components with time-varying frequency, wave-shape function, and amplitude. They coined-out Shape-Adaptive Mode Decomposition (SAMD) algorithm for solving its coefficients of two physiological signals (impedance pneumography and electroencephalography) after applying simulated signals to SAMD. They compared recursive diffeomorphism-based regression, linear regression and multiresolution mode decomposition solutions and ascertained that the proposed SAMD meaningful decomposed with computational efficiency. [28, 29] developed a model verification test in the presence of a random walk-like structure in partial changing frequency of complex-valued sinusoidal signals measured in additive normally distributed noise. The evaluated test makes joint inference of random walk hypothesis tests in economics that link random walk behaviors in time series data, and how the test can be used to account for random walk behaviour in frequency space.

Affirmed by [30], among the problems usually encounter when dealing with oscillatory and wave signals are the decomposition of signals; periodicity transformation in generalization to time-frequency domain; and how to handle non-sinusoidal oscillatory signals. Among the developed algorithms to solve some of the mentioned problems are haemo-dynamic waveform analyses, accelerometer analysis for gait cadence, photoplethysmography (PPG), and detection of motion artifact in PPG. Among the several efforts channeled towards research direction were to simplify oscillatory change detection point in models; handling case when WSF dramatically change from one pattern to another; stretching of wave-shape oscillatory model [31]. Another challenge posed by wave-signals' processing is when each component of the wave-signal has an oscillatory pattern; when the wave-shape function is non-sinusoidal function; or when the oscillatory pattern possessed a non-uniform time variant [32]. In instances that multiple components exist, each component of the wave signal is usually decomposed for extraction of dynamics information, but a widely known and acceptable method or solution for extracting convincing dynamics information is still lacking. Among the recently studied analytic model with complex analysis perspective of analytic signal model are Trigonometric seasonality, Box-Cox transformation, ARIMA errors, Trend and Seasonal components (TBATS), time-varying autoregressive model, wave-shape oscillatory model etc. [33].

In line of wave signal decomposition, this research work will be extending wave signal decomposition to wave-signal-amplitude time variant trigonometry (cosine and sine) regression. The amplitude, phase, and other wave regression coefficients will be estimated using the Ordinary Least Square (OLS) parameter estimation technique. The regression needed sample size (positive integers) for the asymptotic properties that minimizes residual for time variant wave-signal-amplitude trigonometry regression of order "N" will be carried-out via [34]'s criterion of sufficiently needed "N".

2. Methodology

Let $f : K_i \rightarrow \Re$ be a real-valued function satisfying appropriate conditional characterization of $\eta_i (i = 0, \cdots, N) \ni K_i \in [0,\ 2\pi G_i]$, $E(\eta_i) = 0$ and $Var(\eta_i) = \sigma^2$. Then a linear time variant wave-signal-amplitude trigonometry model of cosine and sine function with random errors η_i can be defined as:

$$X = f(G, \Theta) + \eta_i \tag{1}$$

Such that, $\eta_i \approx (0, 1)$, $\Theta = \{a_0, a, b\}$ and $i = 0, \cdots, N$

$$f(G, \Theta) = a_0 + a + bG \tag{2}$$

So, $X_i = a_0 + a + bG_i + \eta_i$ ($X = a_0 + a + bG + \eta$ in matrix form)
Such that,

$$a_0 = \theta_0$$
$$a = \theta_1 \sin\left(2p_i \left({}^{G_i}/_t\right)\right)$$
$$b = \theta_2 \cos\left(2p_i \left({}^{G_i}/_t\right)\right)$$

This implies that,

$$X_i = \theta_0 + \theta_1 \sin\left(2p_i \left({}^{G_i}/_t\right)\right) + \theta_2 G_i \cos\left(2p_i \left({}^{G_i}/_t\right)\right) + \eta_i \tag{3}$$

X_i is a vector of responses.
$\{\theta_0, \theta_1, \theta_2\}$ are the wavy-signal-amplitude trigonometry regression coefficients to be estimated.
G_i is a full rank design matrix of explanatory variable.
"t" is the time variant of the wave that can be in minutes, hours, days, weeks, months, years etc.

3. Parameter estimation of the time variant wavy-signal-amplitude trigonometry regression coefficients via ordinary least square (OLS)

Adopting the OLS parameter estimation technique will make it possible to estimate $\hat{\theta_0}$, $\hat{\theta_1}$ and $\hat{\theta_2}$ via minimizing the sum of squared residuals.

$$X_i = \theta_0 + \theta_1 \sin\left(2p_i \left({}^{G_i}/_t\right)\right) + \theta_2 G_i \cos\left(2p_i \left({}^{G_i}/_t\right)\right) + \eta_i \tag{4}$$

$$RSS = \sum_{i=1}^{N} \widehat{\eta}_i^2 = \sum_{i=1}^{N} \left[X_i - \theta_0 - \theta_1 \sin\left(2p_i \left({}^{G_i}/_t\right)\right) - \theta_2 G_i \cos\left(2p_i \left({}^{G_i}/_t\right)\right)\right]^2 \tag{5}$$

In order to maximize RSS, $\hat{\theta_0}$, $\hat{\theta_1}$ and $\hat{\theta_2}$ will be differentiated and equate their derivations to zero for a system of equations. That is, the least square estimator of θ_0, θ_1 & θ_2, say $\hat{\theta_0}$, $\hat{\theta_1}$ and $\hat{\theta_2}$ must be satisfied,

$$\left.\frac{\partial RSS}{\partial\theta_0}\right|_{\widehat{\theta_0}\,\widehat{\theta_1}\widehat{\theta_2}} = -2\sum_{i=1}^{N}\left[X_i-\theta_0-\theta_1\sin\left(2p_i\left({}^{G_i}\!/_t\right)\right)-\theta_2 G_i\cos\left(2p_i\left({}^{G_i}\!/_t\right)\right)\right] \tag{6}$$

$$\left.\frac{\partial RSS}{\partial\theta_1}\right|_{\widehat{\theta_0}\,\widehat{\theta_1}\widehat{\theta_2}} = -2\sum_{i=1}^{N}\sin\left(2p_i\left({}^{G_i}\!/_t\right)\right)\left[X_i-\theta_0-\theta_1\sin\left(2p_i\left({}^{G_i}\!/_t\right)\right)-\theta_2 G_i\cos\left(2p_i\left({}^{G_i}\!/_t\right)\right)\right] \tag{7}$$

$$\left.\frac{\partial RSS}{\partial\theta_2}\right|_{\widehat{\theta_0}\,\widehat{\theta_1}\widehat{\theta_2}} = -2\sum_{i=1}^{N}G_i\cos\left(2p_i\left({}^{G_i}\!/_t\right)\right)\left[X_i-\theta_0-\theta_1\sin\left(2p_i\left({}^{G_i}\!/_t\right)\right)-\theta_2 G_i\cos\left(2p_i\left({}^{G_i}\!/_t\right)\right)\right] \tag{8}$$

Equating (6), (7), and (8) to zero gives;

$$\sum_{i=1}^{N}\left[X_i-\theta_0-\theta_1\sin\left(2p_i\left({}^{G_i}\!/_t\right)\right)-\theta_2 G_i\cos\left(2p_i\left({}^{G_i}\!/_t\right)\right)\right]=0 \tag{9}$$

$$\sum_{i=1}^{N}\sin\left(2p_i\left({}^{G_i}\!/_t\right)\right)\left[X_i-\theta_0-\theta_1\sin\left(2p_i\left({}^{G_i}\!/_t\right)\right)-\theta_2 G_i\cos\left(2p_i\left({}^{G_i}\!/_t\right)\right)\right]=0 \tag{10}$$

$$\sum_{i=1}^{N}G_i\cos\left(2p_i\left({}^{G_i}\!/_t\right)\right)\left[X_i-\theta_0-\theta_1\sin\left(2p_i\left({}^{G_i}\!/_t\right)\right)-\theta_2 G_i\cos\left(2p_i\left({}^{G_i}\!/_t\right)\right)\right]=0 \tag{11}$$

Equation (9), (10) and (11) are called the Normal equations to be solved for θ_0, θ_1 & θ_2 respectively. Such that, the amplitude is the θ_0 and phase of the model is $\arctan(\theta_1/\theta_2)$, such that wave signal $=\sin\left(2\times\pi\times t\times\left(\widehat{f}+\widehat{\theta}_0+\widehat{\theta}_1+\widehat{\theta}_2\right)\right)$, where $\widehat{f}$ is the frequency. The Normal equations can be subjected to system of equation by [35] for the embedded parameters to be estimated.

4. Selecting the Regression Size Order for the Time Variant Wavy-Signal-Amplitude Trigonometry Regression Function

We shall be studying the method of selecting how large the sample size "N" from a data that best given a good estimator of the point wise of $\widehat{\theta}_0$, $\widehat{\theta}_1$ & $\widehat{\theta}_2$ the model mean square and model performance index. We shall base the sufficiently needed "N" to nullify the variation $\widehat{\sigma}$ that can be ignored on [36]'s criterion of

$$D(N)=\frac{1}{N}\sum_{i=1}^{N}\left[X_i-\theta_0-\theta_1\sin\left(2p_i\left({}^{G_i}\!/_t\right)\right)-\theta_2 G_i\cos\left(2p_i\left({}^{G_i}\!/_t\right)\right)\right]^2+\frac{2N\widehat{\sigma}^2}{n} \tag{12}$$

Where $\overset{\wedge}{\sigma^2}$ is any consistent estimator of the σ_η^2, see [37]. We are particular about the value of $\widehat{N}_n$ that minimize D(N) over the positive integers asymptotic properties of D(N) for selecting the time variant wave-signal-amplitude trigonometry regression of order "N".

Assuming is the minimizer of equation (12), then

$$\int_{0}^{2\pi G_i} \left(f(G,\Theta) - \widehat{f}_{\widehat{N}_n}(G,\Theta)\right)^2 = O_p\left(\frac{1}{\sqrt{n}}\right) \tag{13}$$

This asserts that for the loss function

$$\gamma_n(N) = \int_{0}^{2\pi G_i} \left(f(G,\Theta) - \widehat{f}_{\widehat{N}_n}(G,\Theta)\right)^2 \tag{14}$$

We have $\frac{\gamma_n(\widehat{N}_n)}{\underset{0\le N\le n-1}{Min}\gamma_n(N)}1, \quad as \quad n \to \infty$ (Even if the absolute continuity assumption is not satisfied) If this assumption is satisfied, we have

$$\underset{0\le N\le n-1}{Min} E\left[\int_{0}^{2\pi G_i} \left(f(G,\Theta) - \widehat{f}_{\widehat{N}_n}(G,\Theta)\right)^2\right] = O_p\left(\frac{1}{\sqrt{n}}\right) \tag{15}$$

Its consequence is

$$\underset{0\le N\le n-1}{Min} \int_{0}^{2\pi G_i} \left(f(G,\Theta) - \widehat{f}_{\widehat{N}_n}(G,\Theta)\right)^2 = O_p\left(\frac{1}{\sqrt{n}}\right) \tag{16}$$

This implies that $\gamma_n(N) = O_p\left(\frac{1}{\sqrt{n}}\right)$. That is, any sufficient large size of "n" will be required for estimating $\left\{\theta_0, \theta_1, \theta_2, \sigma^2\right\}$ since $0 \le N \le n-1$. So, any sufficiently needed sample size must be sufficiently large that is far greater than zero.

5. Numerical Analysis

Real-time observations from the Atlantic Marine Energy Test Site (AMETS) data dashboard of wave buoys known as Belmullet Inner (Berth B) and Belmullet Outer (Berth A) are tools that display the real-time performance indicators related to the wave climate. The real-time performance measured by AMETS is being developed by Sustainable Energy Authority of Ireland (SEAI) to facilitate testing of full-scale wave climate and height floating offshore wind technologies in an open ocean harsh met-ocean environment. The full-scale wave climate is the time-variant significant wave height (metre), peak wave direction (in ^oC), and sea temperature (in ^oC) respectively. This research presents an assessment of the wave resource at the AMETS on the west coast of Ireland based on 10-years of recorded data from 2012 to 2022. The primary aim is to provide an assessment of the wave characteristics and resource variability at the two deployment berths.

Table 1. Amplitude Regression Coefficients of Latitudes and Longitudes for Sea Temperature, Peak Direction, and Significant Wave Height for Belmullet Outer (Berth A)

Coefficients	$\hat{\theta}_0$	$\hat{\theta}_1$	$\hat{\theta}_2$	RSE	MRS	ARS	F-statistic	Phase = arctan $(\hat{\theta}_1/\hat{\theta}_2)$	Av. Residual
Latitude Sea Temp. A.	14.7548*** (0.0154)	0.0253*** (0.0149)	0.0763*** (0.0248)	0.0018	0.0140	0.014	1076	0.0001	-0.0012
Longitude Sea Temp.A.	-2.8052*** (0.0474)	-0.055*** (0.0234)	0.3859*** (0.0516)	0.0052	0.0657	0.0657	5330	-0.0026	-0.0016
Latitude Peak Direction.A.	14.7548*** (0.0048)	0.0122*** (0.0069)	-0.0090*** (0.0069)	0.0007	0.0228	0.0134	2.435	-0.0205	-0.0012
Longitude Peak Direction. A.	-2.80523*** (0.0475)	-0.055*** (0.0234)	0.3859*** (0.0515)	0.0052	0.0657	0.0657	5330	-0.0026	-0.0017
Latitude Significant Wave Height.A.	14.7548 *** (0.0049)	0.0040*** (0.0069)	0.0109 ***(0.0069)	0.0007	0.0134	0.0147	1.427	0.0056	0.0020
Longitude Significant Wave Height.A.	-2.8053*** (0.0475)	-0.055*** (0.0234)	0.3859*** (0.0516)	0.0052	0.0657	0.0657	5330	-0.0026	-0.0016

Keys: [a] Temp = Temperature; [b] RSE = Residual Square Error; [c] MRS= Multiple R-Squared; [d] ARS= Adjusted R-Squared

5.1. **Discussion:** Amplitude is the peak value in either the positive or negative direction of full-scale wave climate and its direction in time-variant significant wave height (metre), peak wave direction (in ^oC), and sea temperature (in ^oC). The latitude sea temperature of Belmullet outer (Berth A), latitude peak wave direction Belmullet outer (Berth A) and latitude significant wave height Belmullet outer (Berth A) gave a positive response to the increment of the Atlantic Ocean wave climate of 14.7548 (0.0154), 14.7548 (0.0048), and 14.7548 (0.0049) respectively. In bracket are their p-values, there p-values are significantly less than 0.05 to connote that the amplitude estimates are significantly estimated. This literally means that the sea temperature, peak wave direction and wave height are positively responding and adding to the water and cooling level of the Atlantic Ocean to the north and south of the sea equator. It is to be noted that the amplitude affects the wave height mostly. The longitude sea temperature of Belmullet outer (Berth A), longitude peak wave direction Belmullet outer (Berth A) and longitude significant wave height Belmullet outer (Berth A) gave a negative response to the decrement of the Atlantic Ocean wave climate of -2.8052 (0.0474), -2.80523 (0.0475) and -2.8053 (0.0475) respectively. Concisely, it connotes that the sea temperature, peak wave direction and wave height are negatively reducing the water and cooling level of the Atlantic Ocean to the north and south of the sea equator. In a similar vein, the latitude sea temperature of Belmullet inner (Berth B), latitude peak wave direction Belmullet inner (Berth

Table 2. Amplitude Regression Coefficients of Latitudes and Longitudes for Sea Temperature, Peak Direction, and Significant Wave Height for Belmullet Inner (Berth B)

Coefficients	$\hat{\theta}_0$	$\hat{\theta}_1$	$\hat{\theta}_2$	RSE	MRS	ARS	F-statistic	Phase = arctan $(\hat{\theta}_1/\hat{\theta}_2)$	Av. Residual
Latitude for Sea Temp. B.	14.74124 *** (0.01466)	0.1121*** (0.0143)	0.0567*** (0.0232)	0.0018	0.0724	0.07238	6581	0.0007	0.0018
Longitude for Sea Temp. B.	-2.7618*** (0.05022)	0.0497*** (0.0247)	0.3260*** (0.0546)	0.0016	0.1014	0.1014	9515	0.0004	0.0013
Latitude for Peak Direction.B.	14.7412*** (0.0054)	0.0115*** (0.0076)	-0.0102*** (0.0076)	0.0008	0.0181	0.0092	2.038	-0.0172	0.0015
Longitude for Peak Direction.B.	-2.7618*** (0.0502)	0.0498*** (0.0247)	0.3261*** (0.0546)	0.0016	0.1014	0.1014	9515	0.0003	0.0013
Latitude Significant Wave Height.B.	14.7412*** (0.0114)	-0.0041*** (0.0162)	0.0162*** (0.0162)	0.0017	0.0152	-0.0192	0.4418	-0.0042	0.0020
Longitude Significant Wave Height.B.	-2.7617*** (0.0502)	0.0497*** (0.0247)	0.3260*** (0.0546)	0.0016	0.1014	0.1014	9515	0.0004	0.0013

B) and latitude significant wave height Belmullet inner (Berth B) gave a positive response to the increment of the Atlantic Ocean wave climate of 14.74124 (0.01466), 14.7412 (0.0054), and 14.7412 (0.0114) respectively. The longitude sea temperature of Belmullet outer (Berth A), longitude peak wave direction Belmullet outer (Berth A) and longitude significant wave height Belmullet outer (Berth A) gave a negative response to the decrement of the Atlantic Ocean wave climate of -2.7618 (0.05022), -2.7618 (0.0502) and -2.7617 (0.0502) respectively. It is also noted that all the residual square errors of all the Berths' indexes are relatively small ($RSE < 1$), for all, this means that the time variant wave-signal-amplitude trigonometry regression produced a commendable residual error of η_i.

The frequency (f) value is the number of times a wave goes through in a standard distance or time. If the standard distance is 2π radiant, the frequency is $\sin(f)$ and $\cos(f)$. The wavelength (or period) λ is $2\pi/|f|$. Frequency is the number of cycles in unit time (or length in the spatial domain). From table 3 above, it is only the latitude sea temperature A., latitude peak direction A, latitude significant wave height A, latitude for sea Temp. B, latitude for peak direction B, and latitude significant wave height B gave positive frequencies and signal-waves of (14.8564, 14.776, 14.769, 14.9100, 14.7425, 14.7533) and (0.7506, 0.8013, 0.8055, 0.7142, 0.8209 and 0.8147) respectively.

Table 3. Frequency and Signal-Wave Belmullet Outer (Berth A) and Belmullet Inner (Berth B)

Latitude and Longitude of Belmullets	$\widehat{f}$	$Sin(\widehat{f})$	$Cos(\widehat{f})$	$2\pi/\|f\|$	Signal-Wave
Latitude Sea Temperature A	14.8564	0.7523	-0.6588	0.4231	0.7506
Longitude Sea Temperature A	-2.4743	-0.6189	-0.7855	2.5404	-0.6208
Latitude Peak Direction A	14.776	0.8028	-0.5963	0.4254	0.8013
Longitude Peak Direction A	-2.3859	-0.6858	-0.7278	2.6345	-0.6876
Latitude Significant Wave Height A	14.769	0.8065	-0.5912	0.4256	0.8055
Longitude Significant Wave Height A	-2.4744	-0.6188	-0.7856	2.5403	-08.620
Latitude for Sea Temperature B	14.9100	-0.6982	0.7159	0.4216	0.7142
Longitude for Sea Temperature B	-2.593	-0.5215	-0.8533	2.4241	-0.5236
Latitude for Peak Direction B	14.7425	0.8223	-0.5690	0.4264	0.8209
Longitude for Peak Direction B	-2.3859	0.6858	-0.7278	2.6345	-0.6876
Latitude Significant Wave Height B	14.7533	0.8161	-0.5779	0.4261	0.8147
Longitude Significant Wave Height B	-2.386	0.6857	-0.7279	2.6344	-0.6876

This means that the length occupied in one complete cycle (wavelength) for the stated indexes are 14.8564, 14.776, 14.769, 14.9100, 14.7425 and 14.7533 respectively. The whole berth indexes produced positive wavelength (period) for all.

6. Conclusion

Time variant wavy-signal-amplitude trigonometry regression was extensively studied as a conditional characterization of cosine and sine function with random errors η_i. The parameter estimation of the amplitude, phase, wavelength, wave signal and other regression coefficients were estimated using the Ordinary Least Square (OLS) estimation technique. The needed sample size for robust and efficient of these mentioned estimates and their consistency was carried-out by the Mallow's (1973) criterion. Real-time observations of wave buoys: Belmullet Inner (Berth B) and Belmullet Outer (Berth A) from the Atlantic Marine Energy Test Site (AMETS) of the Atlantic Ocean were subjected to the time variant wavy-signal-amplitude trigonometry regression. The latitude sea temperature of Belmullets (Berth A and B), latitude peak wave direction Belmullets (Berth A and B) and latitude significant wave height Belmullets (Berth A and B) gave a positive response to the increment of the Atlantic Ocean wave climate. In conclusion, the length occupied in one complete cycle (wavelength) for the stated indexes are 14.8564, 14.776, 14.769, 14.9100, 14.7425 and 14.7533 respectively. The whole berth indexes produced positive wavelength (period) for all.

6.1. **Acknowledgments.** We acknowledge the Sustainable Energy Authority of Ireland (SEAI) for releasing the datasets used for us.

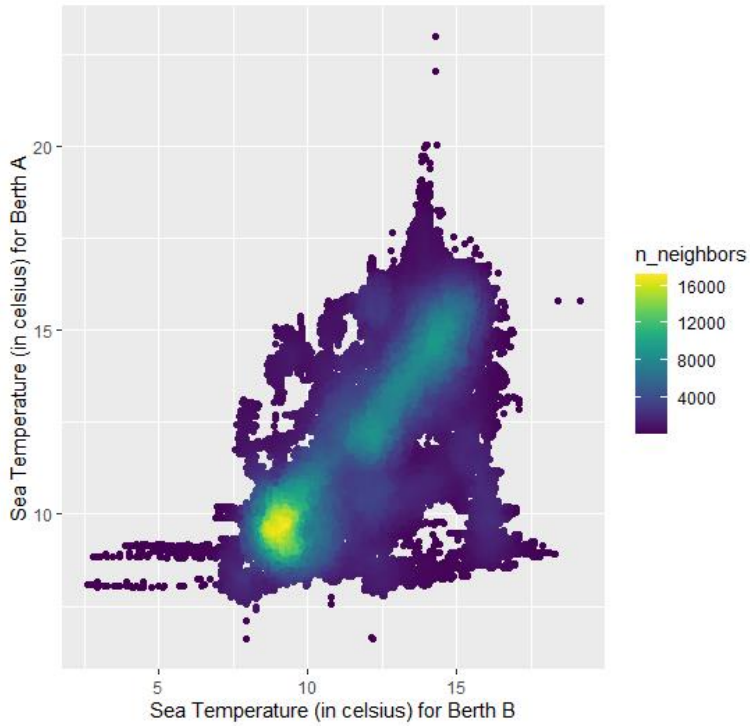

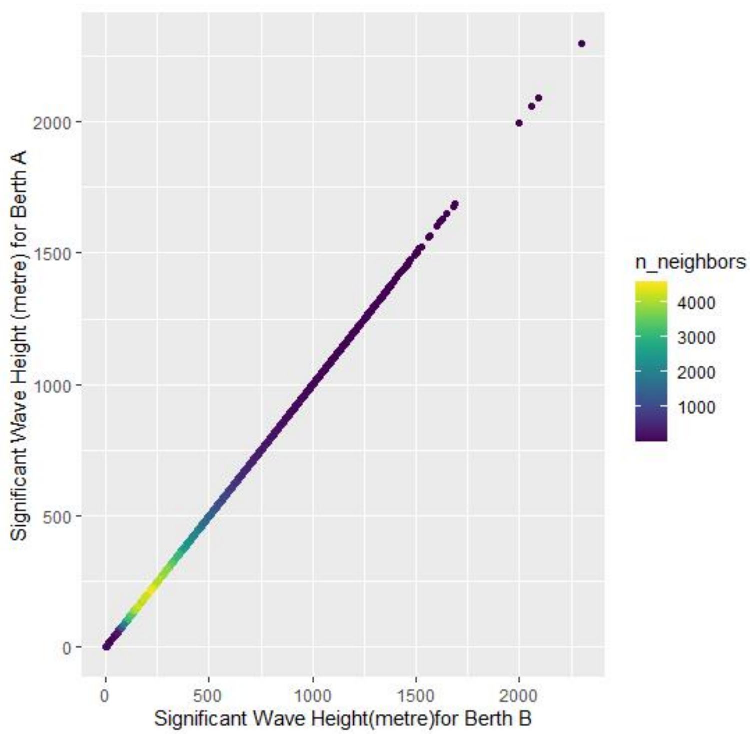

Figure 1. Cross Scatter with Density Plot of Significant Wave Height and Sea Temperature for Belmullet A and B.

References

[1] A. Alian, Y-L. Lo, K. Shelley, H-T, Reconsider phase reconstruction in signals with dynamic periodicity from the modern signal processing perspective. Found. Data Sci. 4(3) (2022) 355–393. https://doi.org/10.3934/fods.2022010.

[2] L. Salmela, G. Han, et al., Feed-forward neural network as nonlinear dynamics integrator for supercontinuum generation, Optim. Lett. 47 (2022) 802–805.

[3] R.O. Olanrewaju, M.A. Jallow, S.A. Olanrewaju, An Analysis of the Atlantic Ocean Random Cosine and Sine Alternate Wavy ARIMA Functions. Int. J. lntell. Syst. Appl. 14(5) (2022) 22-34. https://doi.org/10.5815/ijisa.2022.05.03.

[4] A. Ermolaev, A. Sheveleva, G. Genty, C. Finot, J.M. Dudley, Data driven model discovery of ideal four wave mixing in nonlinear fibre optics. Sci. Rep. 12 (2022) 127-139.

[5] R.O. Olanrewaju, S.A. Olanrewaju, Multinomial Naıve Bayes Classifier: Bayesian versus Nonparametric Classifier Approach. Eur. J. Stat. 2(8) (2022) 1-14. https://doi.org/10.28924/ada/stat.2.8.

[6] J. Berg, K. Nyström, Data-driven discovery of PDEs in complex datasets. J. Comp. Phys. 384 (2019) 239-252.

[7] W. F. Fadel, J.K. Urbanek, S.R. Albertson, X. Li, A.K. Chomistek, J. Harezlak, Differentiating between walking and stair climbing using raw accelerometry data. Stat. Biosci. 11(2) (2019) 334-354.

[8] R.O. Olanrewaju, T.S. Barry, A.H. Muse, A. Habineza, Ornstein-Uhlenbeck process via conflated drive of Brownian motion and Levy process and its application. Math. Theory Model. 11(3) (2021) 12-20.

[9] S. Mallat, A Wavelet Tour of Signal Processing. Academic Press, San Diego, CA (1999).

[10] H-T. Wu, Instantaneous frequency, and wave shape functions. Appl. Comp. Harmon. Anal. 35(2) (2013) 181–199.

[11] C. Hackman, D.B. Sullivan, Time, and frequency measurement. Amer. J. Physics, 63(4) (1995) 306–1076.

[12] R.O. Olanrewaju, On two covariates cosine and sine noisy-wave trigonometry regression of heartbeats. Acad. J. Appl. Math. Sci. 5(10) (2019) 140-149.https://doi.org/10.32861/ajams.510.140.149.

[13] M.A. Colominas, H.-T. Wu, An iterative warping and clustering algorithm to estimate multiple wave-shape functions from a nonstationary oscillatory signal, IEEE Trans. Signal Process. 71 (2023) 701-712. https://doi.org/10.1109/tsp.2023.3252883.

[14] U. Fasel, J.N. Kutz, B.W. Brunton, S.L. Brunton, Ensemble Robust sparse model discovery in the low-data, high-noise limit, with active learning and control. Proc. R. Soc. A. 478 (2022) 190-202.

[15] R.O. Olanrewaju, Bayesian approach: an alternative to periodogram and time axes estimation for known and unknown white noise. International Journal of Mathematical Sciences and Computing, 2(5) (2018) 22-33. https://doi.org/10.5815/ijmsc.2018.02.03.

[16] Y-T. Lin, J. Malik, H-T. Wu, Wave-shape oscillatory model for nonstationary periodic time series analysis. Found. Data Sci. 3(2) (2021) 99-131.

[17] R.O. Olanrewaju, Penalized likelihood estimation of gamma distributed response variable via corrected solution of regression coefficient. J. Mod. Appl. Stat. Meth. 9(1) (2021), 1-18.https://doi.org/10.22237/jmasm/16085527.

[18] T. Qin, K. Wu, D. Xiu, Data driven governing equations approximation using deep neural networks. J. Comp. Phys. 395 (2019) 620–635.

[19] J. Ruiz, M.A. Colominas, Wave-shape function model order estimation by trigonometric regression. Signal Process. 197 (2022) 108-543.

[20] R.O. Olanrewaju, J.F. Ojo, Non-convex penalized estimation of count data responses via generalized linear model (GLM). Asian J. Fuzzy Appl. Math. 8(3) (2020) 27-38.

[21] P.W. Hatfeld, Data-driven future of high-energy-density physics. Nature, 593 (2021) 351–361.

[22] O. Skliar, V. Medina, R.E. Monge, A New Method for the analysis of signals: the square wave method. Rev. Mat.: Teor. Apl. 15(2) (2008) 109-129.

[23] S.A. Phillips, E.A. Ayanlowo, R.O. Olanrewaju, O. Fatoki, Jeffrey's prior of unknwon sinusoidal noise model via Cramer-Rao lower bound. Int. J. Comp. Sci. Math. 13(5) (2019) 117-122.

[24] Y. Cui, E.I. Sfakianakis, Detectable gravitational wave signals from inflationary preheating. arXiv:2112.00762v1. (2021).

[25] L. Su, H-T. Wu, Extract fetal ECG from single-lead abdominal ECG by de-shape short time fourier transform and nonlocal median. Front. Appl. Math. Stat. 3(2) (2017) 145–436.

[26] J.F. Ojo Johnson, A.O. Olubiyi, and R.O. Olanrewaju, Empirical distribution of emissions from commercial motorcycles (Okada) and motor vehicles in Abeokuta, Nigeria. Int. J. Environ. Bioenergy, 14(1) (2019) 20-39.

[27] D-H. Pham, S. Meignen, High-order synchrosqueezing transform for multi-component signals analysis - with an application to gravitational-wave signal. IEEE Trans. Signal Process. 65(12) (2017) 3168–3178.

[28] C.A. Marcello, H-T. Wu, Decomposing non-stationary signals with time-varying wave-shape functions. IEEE Trans. Signal Process. 69 (2021) 5094-5104. https://doi.org/10.1109/TSP.2021.3108678.

[29] R.O. Olanrewaju, Integer-valued time series model via generalized linear models technique of estimation. Int. Ann. Sci. 4(1) (2018) 35-43. https://doi.org/10.21467/ias.4.1.35-43.

[30] S. Abramson, W. Moran, R. Evans, A. Melatos, Testing for a random walk structure in the frequency evolution of a tone in noise. Sensors, 22 (2022) 6103. https://doi.org/10.3390/s22166103.

[31] R.O. Olanrewaju, On the efficiency and robustness of commingle Wiener and Levy driven processes for Vasciek model. Int. J. Math. Comp. Sci. 12(11) (2018) 228-233.

[32] R.O. Olanrewaju, L.O. Adekola, E. Oseni, S.A. Phillips, A.A. Oyinloye, Disintegration of price ordered probit model: an application to prices of cereal crops in Nigeria. Afr. J. Appl. Stat. 7(1) (2020) 781-804. https://doi.org/10.16929/ajas/2020.781.242.

[33] A.K. Maity, A. Veeraraghavan, A. Sabharwal, Motion: Model-based detection of motion artifacts in photoplethysmography signals. Biomed. Signal Process. Control, 75 (2022) 103-632.

[34] S. Marchesini, Y-C. Tu, H-T. Wu, Alternating projection, ptycho-graphic imaging, and phase synchronization. Appl. Comp. Harmon. Anal. 41(3) (2016) 815–851.

[35] G.E. Karniadakis, Physics-informed machine learning. Nat. Rev. Phys. 3 (2021) 422-440.

[36] C.L. Mallows, Some comments on Cp. Technometrics, 15(4) (1973) 661-675. https://doi.org/10.2307/1267380JSTOR1267380.

[37] C.S. Wong, Statistical inference for some nonlinear time series models, Ph.D thesis, University of Hong Kong, Hong Kong, (1998).

[38] W. Cui, W. Wei, Strong consistency of kernel regression estimate. Open Journal of Statistics, 3(3) (2013) 179-182. https://doi.org/10.4236/ojs.2013.33020.

7. Appendix

Appendix 1:

For some conditions on Fourier series satisfying $s(t) = \sum_{\gamma \in Z} \widehat{s}(\gamma) e^{i\gamma 2\pi t}$, where $\widehat{s}(\gamma)$ are the Fourier parameters. $f(t) = A(t)s(\phi(t))$ must fulfill the following slowing and time-varying conditions:

1. $\left\|\phi''\right\|_{\infty} \leq G$, with $G \geq 0$
2. For $\omega > 0$, $\left|A'(t)\right| < \omega\phi'(t)$ and $\left|\phi''(t)\right| < \omega\phi'(t)$